Biochemistry
Article
Cite This: Biochemistry XXXX, XXX, XXX−XXX
pubs.acs.org/biochemistry

Design of Small Molecules That Compete with Nucleotide Binding to an Engineered Oncogenic KRAS Allele

Yan Zhang,[†] Marie-Hélène Larraufie,[‡] Leila Musavi,[‡] Hemanth Akkiraju,[‡,§] Lewis M. Brown,[‡,§] and Brent R. Stockwell*[,†,‡]

[†]Department of Chemistry and [‡]Department of Biological Sciences, Columbia University, Northwest Corner Building, 12th Floor, MC 4846, 550 West 120th Street, New York, New York 10027, United States

[§]Quantitative Proteomics and Metabolomics Center, Columbia University, New York, New York 10027, United States

Supporting Information

ABSTRACT: *RAS* mutations are found in 30% of all human cancers, with *KRAS* the most frequently mutated among the three *RAS* isoforms (*KRAS*, *NRAS*, and *HRAS*). However, directly targeting oncogenic KRAS with small molecules in the nucleotide-binding site has been difficult because of the high affinity of KRAS for GDP and GTP. We designed an engineered allele of KRAS and a covalent inhibitor that competes for GTP and GDP. This ligand−receptor combination demonstrates that the high affinity of GTP and GDP for RAS proteins can be overcome with a covalent inhibitor and a suitably engineered binding site. The covalent inhibitor irreversibly modifies the protein at the engineered nucleotide-binding site and is able to compete with GDP and GTP. This provides a new tool for studying KRAS function and suggests strategies for targeting the nucleotide-binding site of oncogenic RAS proteins.

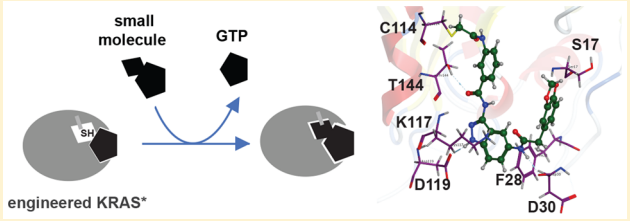

The RAS superfamily of small GTPases consists of more than 150 GTP-binding proteins that play key roles in the regulation of cell growth and survival.[1] There is speculation that several members of this family, including RAS, RAC1, RHOA, and RHEB proteins, could serve as effective targets in multiple diseases. *RAS* mutations are found in 30% of human cancers, with *KRAS* being the most frequently mutated (86%) among the three *RAS* isoforms (*KRAS*, *NRAS*, and *HRAS*).[2] It has been postulated that KRAS is essential for tumor maintenance, but not for normal adult physiology, thus rendering inhibition of KRAS a "Holey Grail" in cancer therapy. Recently, the discoveries of a pan-RAS inhibitor[3] and $KRAS^{G12C}$ covalent inhibitors[4,5] showed the feasibility of directly targeting RAS protein in some cases. However, pharmacological and genetic validation of the therapeutic index associated with targeting RAS and other small GTPases requires further investigation.

The KRAS protein functions as a molecular switch, cycling between a GTP-bound active state and a GDP-bound inactive state. Oncogenic mutations in KRAS impair its intrinsic and GAP-mediated GTPase function, resulting in the accumulation of KRAS-GTP that constitutively activates KRAS downstream signaling. Pharmacological validation of KRAS and other small GTPases as therapeutic targets is difficult because of their picomolar affinity for GTP and GDP. Thus, creating a potent and selective small-molecule inhibitor for these proteins is challenging.

Generating engineered, inhibitable alleles of proteins to validate targets has proven to be successful for kinases and other proteins.[6−15] The essence of this strategy resides in the design of engineered alleles of the protein of interest that are sensitized to small-molecule inhibition, while being functionally indistinguishable from wild-type counterparts (Figure 1A). Treatment with a complementary small-molecule probe can then provide selective, rapid, and dose-dependent inactivation of the protein of interest. More recently, Shah and co-workers reported a strategy for the selective inhibition and activation of an engineered H-Ras mutant by unnatural GDP and GTP analogues.[16] However, future applications of that study were limited by the use of GDP analogues as molecular probes, which are inherently non-cell-permeable and not selective. Moreover, that study did not address the feasibility of designing a druglike small molecule that targets engineered small GTPases.

We aimed to address this issue by testing whether we could design a cell-permeable small-molecule probe that would allow us to test the effects of pharmacological inhibition of suitably engineered small GTPases. We focused on the design of small molecules capable of inhibiting an engineered mutant allele of oncogenic KRAS (termed KRAS*). We were concerned that mutation of key conserved residues in KRAS might alter its natural nucleotide selectivity and important protein−protein interactions, making the mutant activated in a GEF-independent way and causing loss of the switch function,[16−18] as first suggested for RAS (N116I).[19] Shah and co-workers have reported, however, that H-RAS (L19A and N116A) mutants remain as fully functional as the wild-type enzyme.[16] We also demonstrated that the engineered inhibitable KRAS* allele we designed has an effective "on" and "off" switch mechanism and fully functions in cells.

Received: November 2, 2017
Revised: December 16, 2017
Published: January 9, 2018

DOI: 10.1021/acs.biochem.7b01113
Biochemistry XXXX, XXX, XXX−XXX

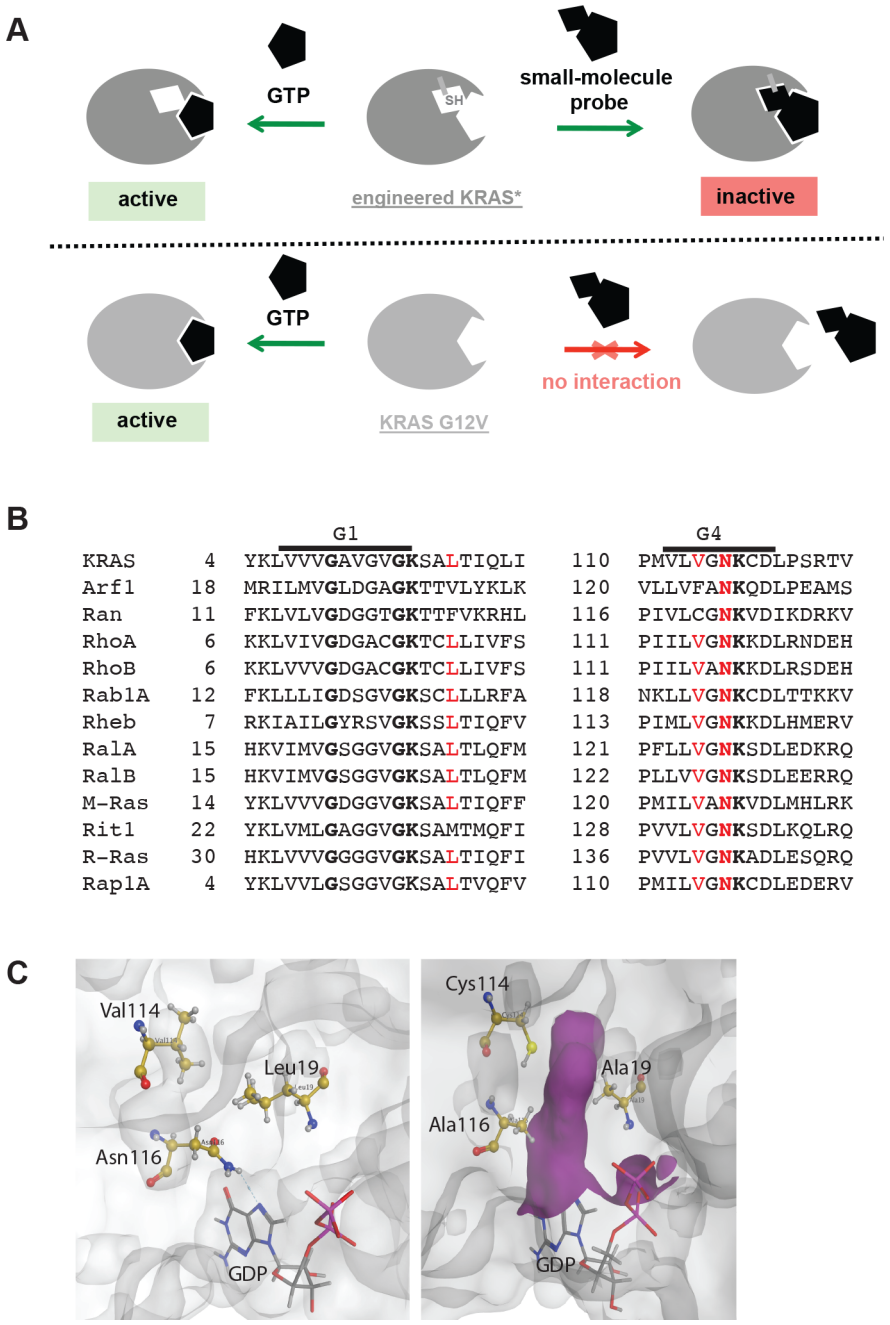

Figure 1. Design of the engineered KRAS allele. (A) The engineered KRAS* harbors an enlarged pocket and a cysteine residue, which enables the design of a covalent molecule that selectively targets KRAS* over KRAS^{G12V}. (B) Sequence alignment of RAS and members of the small GTPase superfamily (conserved residues are in bold). (C) Representation of KRAS G12V (Protein Data Bank entry 4TQ9) and engineered KRAS* (structure minimized using Schrödinger Prime).

We report herein the computational design of a mutant engineered oncogenic allele of KRAS bearing an enlarged nucleotide-binding site and a cysteine residue that can serve as a site for covalent targeting. We found that this mutant KRAS* was functionally indistinguishable from KRAS^{G12V} but could be selectively inhibited by a computationally designed covalent inhibitor.

RESULTS

Rational Design of the KRAS Allele. Small GTPases in the RAS family have a conserved binding site and share similar nucleotide-binding pockets[20](Figure 1B). Shah and co-workers demonstrated that mutation of L19 and N116, located on the backside of the HRAS GTP-binding site, to smaller alanine residues allowed access to a buried hydrophobic cavity. The crystal structure of KRAS^{G12V} in the GDP-bound conformation [Protein Data Bank (PDB) entry 4TQ9[21]] was used as a template to model the influence of point mutations in the nucleotide-binding site. Prime and BioLuminate (Schrödinger) were used to calculate the change in structure and stability of the protein after the introduction of mutations (Table S1). Residues 19 and 116 were mutated *in silico*, and all residues within 10 Å of either mutation were minimized. A new hydrophobic cavity that was 3 Å wide and 10 Å long appeared in the nucleotide-binding site (Figure 1C). We next wished to introduce a cysteine residue into the hydrophobic pocket that could then be used as a handle for covalent inhibition.[3] Indeed, we envisioned that the use of covalent inhibitors

DOI: 10.1021/acs.biochem.7b01113
Biochemistry XXXX, XXX, XXX−XXX

might be the key to coping efficiently with the high cellular concentration of GTP (0.5 mM).[22] For that purpose, a cysteine residue (C114) that could be targeted by electrophilic moieties was installed in the backside of the engineered hydrophobic pocket. The stability of the engineered protein (KRAS*^{G12VL19AN116AV114C}, termed KRAS*) was predicted to have decreased energy of 52.96 kcal/mol. The predicted structure of the engineered protein showed that C114 was oriented to perform a nucleophilic attack on electrophilic moieties in the pocket (Figure 1C). Importantly, the three mutated residues in KRAS* are in a conserved site among the GTPases, so they could potentially be translated to other members of the family.

Function of the Engineered KRAS Allele. To verify that the engineered mutant allele functions well as a "switch", KRAS* was loaded with GDP or GTP and incubated with the RAF1 RBD (RAS-binding domain) protein attached to glutathione Sepharose beads. The unbound KRAS* was removed during the washing step, while the bound KRAS* was quantified by immunoblotting with the anti-RAS antibody. As expected, the RAF1 RBD specifically bound to GTP-loaded KRAS* but not GDP-loaded KRAS* (Figure 2A). To prove that the KRAS* is not a nucleotide-free analogue of RAS as suggested for HRAS(N116I), we tested the binding of GDP and GTP by KRAS* and KRAS^{G12V} (Figure 2B,C). Both KRAS* and KRAS^{G12V} were nucleotide-exchanged with BODIPY-GTP, a fluorescent analogue of GTP that has a high polarization value when it binds with protein and a low polarization value in the unbound form. BODIPY-GTP was displaced by GDP or GTP in both KRAS* and KRAS^{G12V}, indicating KRAS* retains nucleotide selectivity. Compared with KRAS^{G12V}, the faster nucleotide exchange rate of BODIPY-GTP with GTP or GDP might come from the low binding affinity of KRAS* for BODIPY-GTP.

To further verify KRAS* function in cells, we used RAS-less MEFs. *K-Ras^{lox}*(*H-Ras$^{-/-}$;N-Ras$^{-/-}$;K-Ras$^{lox/lox}$;RERTn$^{ert/ert}$*) mouse embryonic fibroblasts (MEFs) were stably transfected with *KRAS** or *KRAS^{G12V}* alleles.[23] The MEFs were generated to carry null *HRAS* and *NRAS* alleles along with a floxed *KRAS* locus and a knocked-in inducible Cre recombinase. After transfection, 4-hydroxytamoxifen was used to induce Cre recombinase, resulting in the complete elimination of the endogenous *KRAS* gene after 2 weeks (termed *KRAS** MEFs and *KRAS^{G12V}* MEFs) (Figure S1). The ability of KRAS* to activate RAF/MEK/ERK signaling was examined by measuring the abundance of phosphorylated ERK (pERK) and phosphorylated AKT (pAKT) in the transfected cell lines. Following EGF treatment, pERK and pAKT levels were increased in the transfected cell lines (Figure 2D), demonstrating that the engineered mutations did not prevent KRAS* from activating effector proteins. The EGF-dependent signal in *KRAS** MEFs also revealed that its binding to GTP was not GEF-independent as suggested for RAS (D119N).[18] KRAS mRNA levels were measured in the transfected cell lines by quantitative polymerase chain reaction. We found that the *KRAS** mRNA was more abundant than the *KRAS^{G12V}* mRNA (Figure 2E). Compared with the similar protein level of KRAS in *KRAS** MEFs and *KRAS^{G12V}* MEFs (Figure 2A), that might exist because KRAS* is less stable than KRAS^{G12V} (Figure S1), which provides an advantage for rapidly inducing and removing this engineered protein from cells.

Design of Small-Molecule Ligands. A GDP-bound KRAS^{G12V} crystal structure (PDB entry 4TQ9) was used to design compounds that covalently lock KRAS* in the GDP-bound state, inactivating its signaling function. KRAS^{G12V} was mutated *in silico* to KRAS*, and the engineered structure was refined by Schrödinger Protein Preparation Wizard for docking studies. A fragment-based design strategy was applied in the search for a covalent inhibitor,[24] and two series of covalent inhibitors were designed and synthesized; 177911 fragments (SI Software) were screened using the Schrödinger Glide program, and the top-ranked fragments were used as scaffolds for further design. The first series of inhibitors (Figure 3A and Figure S2) harbor a carboxylic acid group, which is predicted to interact with the magnesium ion and multiple residues in the GTP-binding pocket, thus giving a high predicted binding affinity (as good as −12 for Glidescore). These inhibitors had high predicted binding affinities for the KRAS* protein (Figure S3) but low cellular activity (Table S3), making it difficult to study the KRAS therapeutic index in cells. Compound **7** had two carboxylic acid groups and, thus, likely could not penetrate cell membranes (Table S2). Esterification of carboxylic acid groups can make compounds more cell membrane-permeable; the measured levels of cellular accumulation of compounds **6** and **8** were 3.9- and 15.6-fold (Table S2), respectively. The low cellular activity might thus derive from their inability to block KRAS−effector interactions in cells.

We then found that the conserved aspartate residue D119 is a key residue determining the specificity for GTP over other nucleotides through hydrogen bonding. We reasoned that the discovery of a compound that can form hydrogen bonds with D119 is thus important for a successful design. H-Bond constraints were applied to D119 in fragment screens for a second inhibitor design series. Top-ranked fragments without carboxylic acid groups were tested in a fluorescence polarization assay to measure the binding affinity for KRAS*. We found that an indazole fragment **G**, with a docking score of −7.1 (Figure 3B and Figure S2), could compete with GTP binding for KRAS in vitro in the range of 100 μM (Figure S4) and was chosen as a scaffold for further design. As a next step, the hydrophobic pocket of the engineered allele was targeted by attaching a lipophilic group (Figure 3B) to the appropriate site on fragment **G**. This produced compound **G***, which had a more favorable docking score of −9.1, compared to a score of −7.1 for compound **G** (note that the Glide docking score is a log scale, so this predicted a 100-fold improvement in affinity). On the basis of the structure of compound **G**, a number of covalent inhibitors with electrophile warheads at different positions were designed and evaluated using Schrödinger's Covalent Docking program.[25] This showed that having a 2-chloroacetamide electrophile at the *meta* position (compound YZ0468) had the best predicted affinity score *in silico* (docking structure shown in Figure 3A). On the basis of this indazole scaffold, a customized compound library employing amide coupling, reductive aminations, and cross coupling reactions was created (Figure 3C) and evaluated using Schrödinger's Glide Docking and Covalent Docking programs. The top-scoring compounds were synthesized and tested in the fluorescence polarization assay to further assess inhibition activity.

Synthesis of Covalent KRAS* Inhibitors. A set of promising covalent small-molecule inhibitors was thus synthesized (Table S3). As an example, the synthetic route developed for compound YZ0711 is illustrated in Figure 3D. The indazole scaffold was synthesized by heating 2-fluoro-5-nitrobenzonitrile and hydrazine monohydrate in refluxing ethanol followed by the selective BOC protection of the N-1 position of the indazole and subsequent palladium-catalyzed hydrogenation.[26] The resulting diaminoindazole could be acylated selectively at the C-5 amine using an acid chloride. In the next step, the C-3 amine was acylated in pyridine to yield compound **4**. Catalytic hydrogenation of the nitro group in compound **4** followed by acylation of the resulting

DOI: 10.1021/acs.biochem.7b01113
Biochemistry XXXX, XXX, XXX−XXX

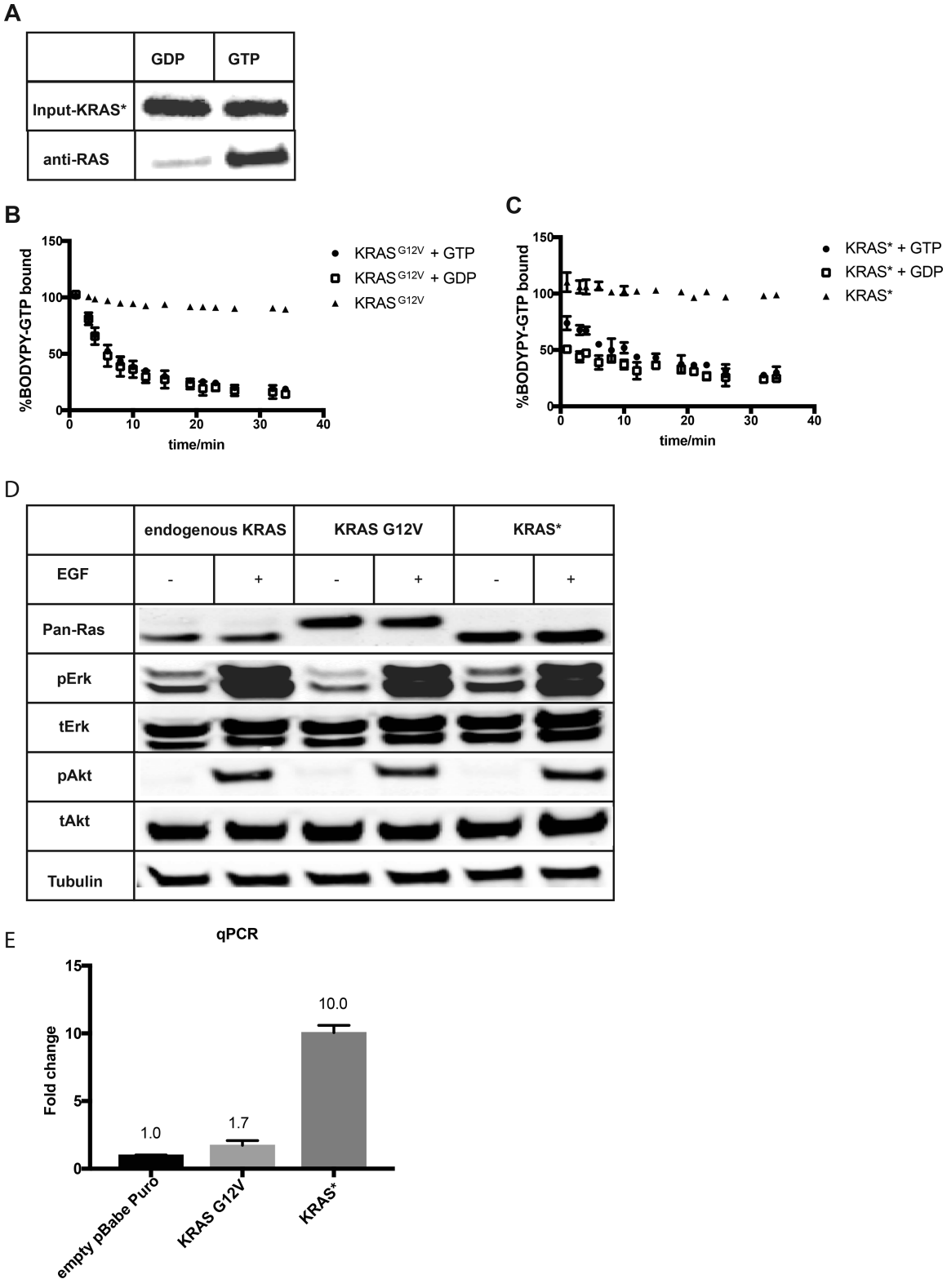

Figure 2. Establishment of engineered KRAS knock-in cell lines. (A) The RAF RBD can selectively pull down GTP-loaded KRAS* but not GDP-loaded KRAS*. (B) Amount of exchanged GDP and GTP in $KRAS^{G12V}$ as a function of time. (C) Amount of exchanged GDP and GTP in KRAS* as a function of time. (D) Western blot indicating the overexpression of RAS in $KRAS^{G12V}$ MEFs and *KRAS** MEFs. RAS downstream signaling was activated upon EGF treatment. The endogenous KRAS MEFs are MEFs transfected with the empty pBabe vector but without hydroxygamoxifen selection. The transfected pBabe puro KRAS G12V vector has a FLAG tag (N-terminal on the insert) causing it to migrate slower through the gel than endogenous KRAS and KRAS* do (KRAS* without the FLAG tag was inserted into the pBabe vector). (E) Quantitative polymerase chain reaction shows overexpression of KRAS in the transfected cell lines.

aniline with chloroacetyl chloride and selective deprotection of the BOC group provided the desired product.

Biophysical Measurements. We developed an *in vitro* fluorescence polarization assay to test the ability of small molecules

DOI: 10.1021/acs.biochem.7b01113
Biochemistry XXXX, XXX, XXX−XXX

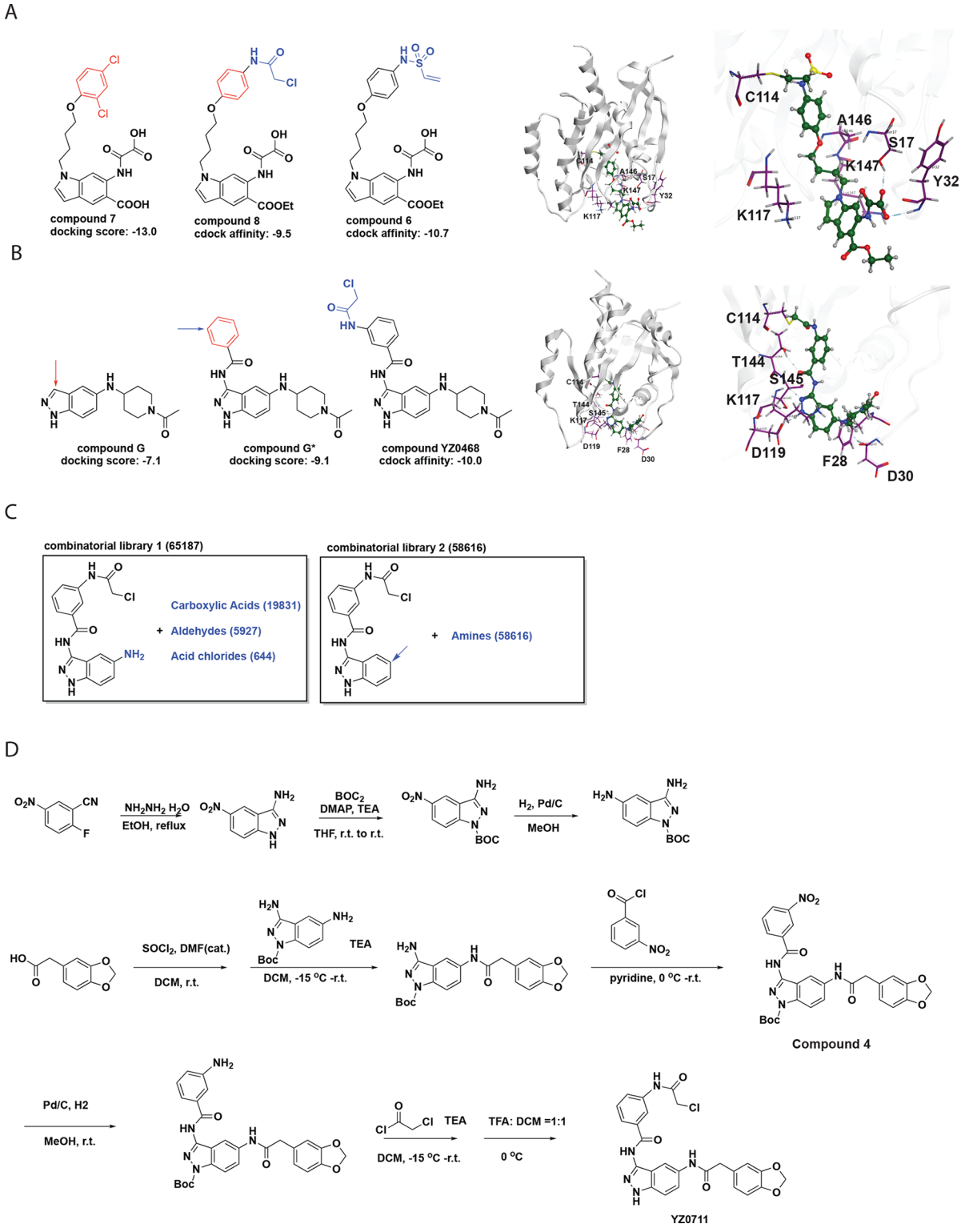

Figure 3. Design and synthesis of covalent inhibitors. (A) Design of a first series of small molecules and representation of the proposed binding mode of compound **6** in KRAS*. The benzyl moiety is designed to target the engineered hydrophobic pocket. Electrophile warheads are designed to covalently react with C114. Covalent docking of compound **6** in KRAS* showed favorable formation of a covalent bond between C114 and the vinyl sulfone moiety (the docking pose is shown). The ligand is predicted to form a hydrogen bond interaction with residues A146, C114, S17, and Y32 and π−cation interaction with residues K117 and K147 (docking was conducted by Schrödinger's Covalent Docking program). (B) Design of a second series of small molecules and representation of the proposed binding mode of compound YZ0468 in KRAS*. Covalent docking of compound YZ0468 in KRAS* showed favorable formation of a covalent bond between C114 and the chloroacetyl moiety (the docking pose is shown). The ligand is predicted to form a hydrogen bond interaction with residues D30, D119, T144, and S145, π−cation interaction with residue K117, and π−π interaction with residue F28. (C) Combinatorial library design (created by MOE) (libraries of carboxylic acids, aldehydes, acid chlorides, and amines are collected from Sigma-Aldrich). (D) Synthesis of compound YZ0711.

DOI: 10.1021/acs.biochem.7b01113
Biochemistry XXXX, XXX, XXX−XXX

to displace BODIPY-GTP, a fluorescent analogue of GTP. In this assay, test compounds that were able to competitively replace BODIPY-GTP bound to KRAS* resulted in a decrease in the polarization of BODIPY-GTP (Figure 4A).

The designed covalent inhibitors and noncovalent inhibitors were able to compete with fluorescent GTP binding for the engineered mutant, but not for KRAS^{G12V} (Figure 4 and Figure S5), thus satisfying the selectivity criterion. In addition, inhibitor

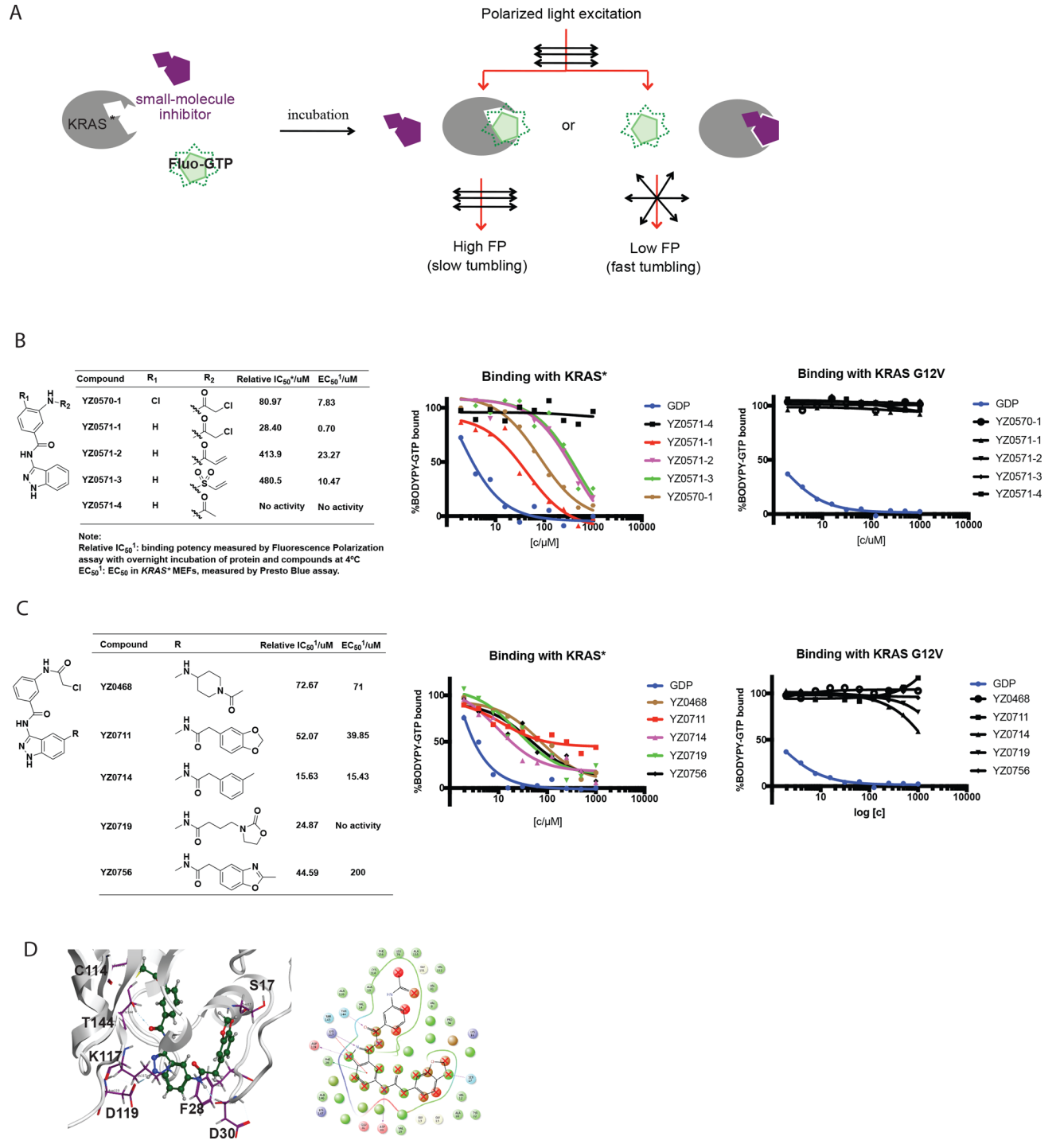

Figure 4. Fluorescent polarization assay showing the competitive displacement of GDP in KRAS* protein. (A) Fluoro-GTP binds in the GTP-binding site to yield a high fluorescence polarization (FP) value. With the displacement of small-molecule inhibitors, fluoro-GTP shows a small FP value. (B) Structures and activities of selected covalent inhibitors. Covalent inhibitors selectively occupy the GTP-binding pocket of KRAS*, but not that of KRAS^{G12V} protein. Compound YZ0571-1, bearing a 2-chloroacetyl chloride moiety, has optimal activity in the fluorescence polarization assay and cell viability assays. (C) Structures and activities of selected covalent inhibitors. Covalent inhibitors selectively displace GDP from KRAS* protein, but not from KRAS^{G12V} protein. (D) Compound YZ011 is covalently docked in KRAS* (the docking pose is shown). WaterMap shows the thermodynamic properties of the hydration site around the protein active site. Stable hydration sites (ΔG < 3 kcal/mol) are colored green; significantly unstable hydration sites (ΔG > 5 kcal/mol) are colored red, and moderately unstable sites (3 kcal/mol < ΔG < 5 kcal/mol) are colored brown. Compound YZ0711 displaces nearly all high-energy waters in the binding site.

DOI: 10.1021/acs.biochem.7b01113
Biochemistry XXXX, XXX, XXX−XXX

binding was catalyzed by EDTA but not SOS1, a guanine nucleotide exchange factor that promotes guanine nucleotide exchange (Figure S5). Compared with compounds bearing acrylamide and vinyl sulfonate warheads, compounds bearing a chloroacetyl warhead were more able to bind to KRAS* (Figure 4B). This might result from the relatively small pocket in KRAS*. Indeed, an extra chloro group on the benzyl moiety of YZ0571-1 decreased potency, consistent with a small available space in the binding site. In addition, a noncovalent analogue (YZ0571-4) was not able to displace BODIPY-GTP. On the basis of this result, a series of covalent inhibitors incorporating chloroacetyl warheads were synthesized. Compounds YZ0714 and YZ0719 had binding affinities comparable to thta of YZ0571-1. Compound YZ0719 has low activity in a cell viability assay, which might result from its low cell membrane permeability (Table S2). Compound YZ0711 had the best selectivity at inhibiting KRAS signaling among these electrophiles (data not shown) and was selected for further analysis.

WaterMap (Schrödinger), which calculates thermodynamics associated with water hydration sites in protein active sites,[27,28] showed that compound YZ0711 displaced nearly all high-energy hydration sites in the nucleotide-binding site of KRAS* (Figure 4D and Figure S6). This result indicated possible favorable binding between compound YZ0711 and KRAS* protein.

Mass Spectrometry Analysis of Covalent Binding. To determine whether compound YZ0711 could covalently bind to KRAS*, purified KRAS* (20 μM) was incubated with 200 μM YZ0711 and 1 mM EDTA overnight at 4 °C. The protein was then labeled with iodoacetamide and digested with trypsin. The resulting peptides were analyzed by nano liquid chromatography and mass spectrometry (LC−MS). LC−MS analysis revealed a modification of peptide R.VKDSEDVPMVLCGAK.C (103−117) with YZ0711 at a cysteine (C114) or lysine (K117) residue (Figure 5A). Peptide R.VKDSEDVPMVLVGNK.C (103−117) lacking cysteine but containing lysine in KRAS^{G12V} was not modified with YZ0711

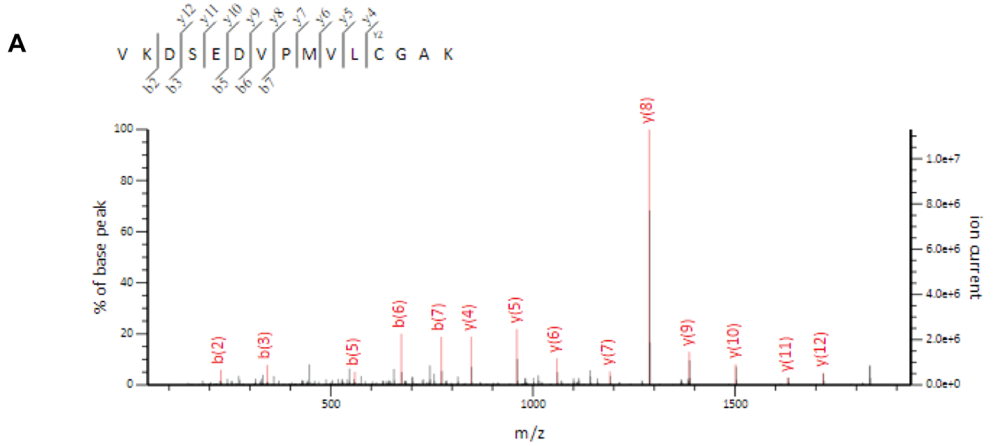

Score	Mr(calc)	Delta	Sequence
74.3	2058.9179	0.0038	VKDSEDVPMVLCGAK +YZ0711_Lysine (K)
74.3	2058.9179	0.0038	VKDSEDVPMVLCGAK +YZ0711_Cysteine(C)

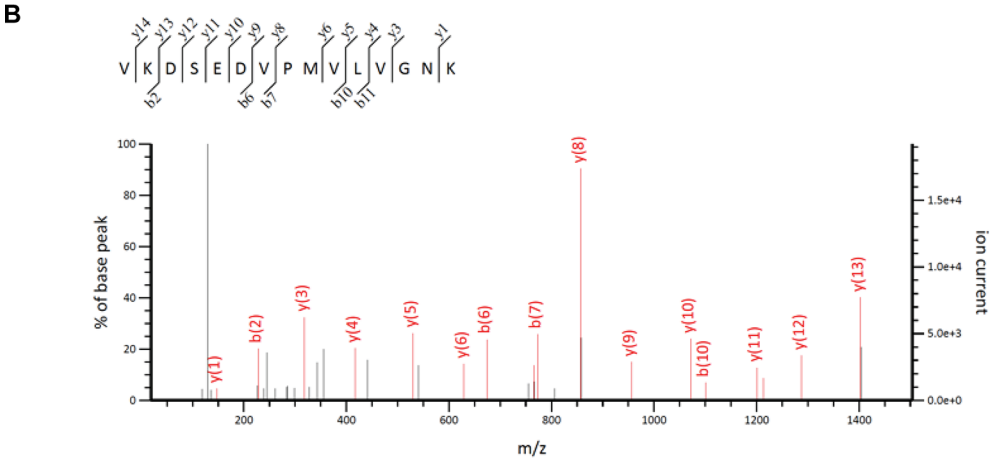

Score	Mr(calc)	Delta	Sequence
98.6	1628.8444	0.0090	VKDSEDVPMVLVGNK
82.5	1628.8444	0.0090	VKDSEDVPMVLVGNK

Figure 5. YZ0711 covalently labels KRAS* but not KRAS G12V. Liquid chromatography and mass spectrometry of peptide 103−117 in KRAS* (A) and KRAS^{G12V} (B). Peptide 103−117 in KRAS* was detected to be labeled by YZ0711 at either a lysine or cysteine. No labeling was detected in peptide 103−117 in KRAS^{G12V}.

DOI: 10.1021/acs.biochem.7b01113
Biochemistry XXXX, XXX, XXX−XXX

(Figure 5B), indicating that YZ0711 modification was exclusive to C114 in KRAS*. The YZ0711 modification at cysteine was strongly supported by 19 Mascot queries returning the sequence R.VKDSEDVPMVLCGAK.C consistent with the modification with YZ0711 at C114. These queries had an average ion score of 37 with RMS error of 3.8 ppm for precursors, and RMS error of 4.3 ppm for product ions. These peptide identifications were supported by an average of 9.7 fragment ions per peptide.

Cell-Based Assay. The *KRAS** MEFs and *KRAS*^{G12V} MEFs described above were used in cellular assays. We investigated

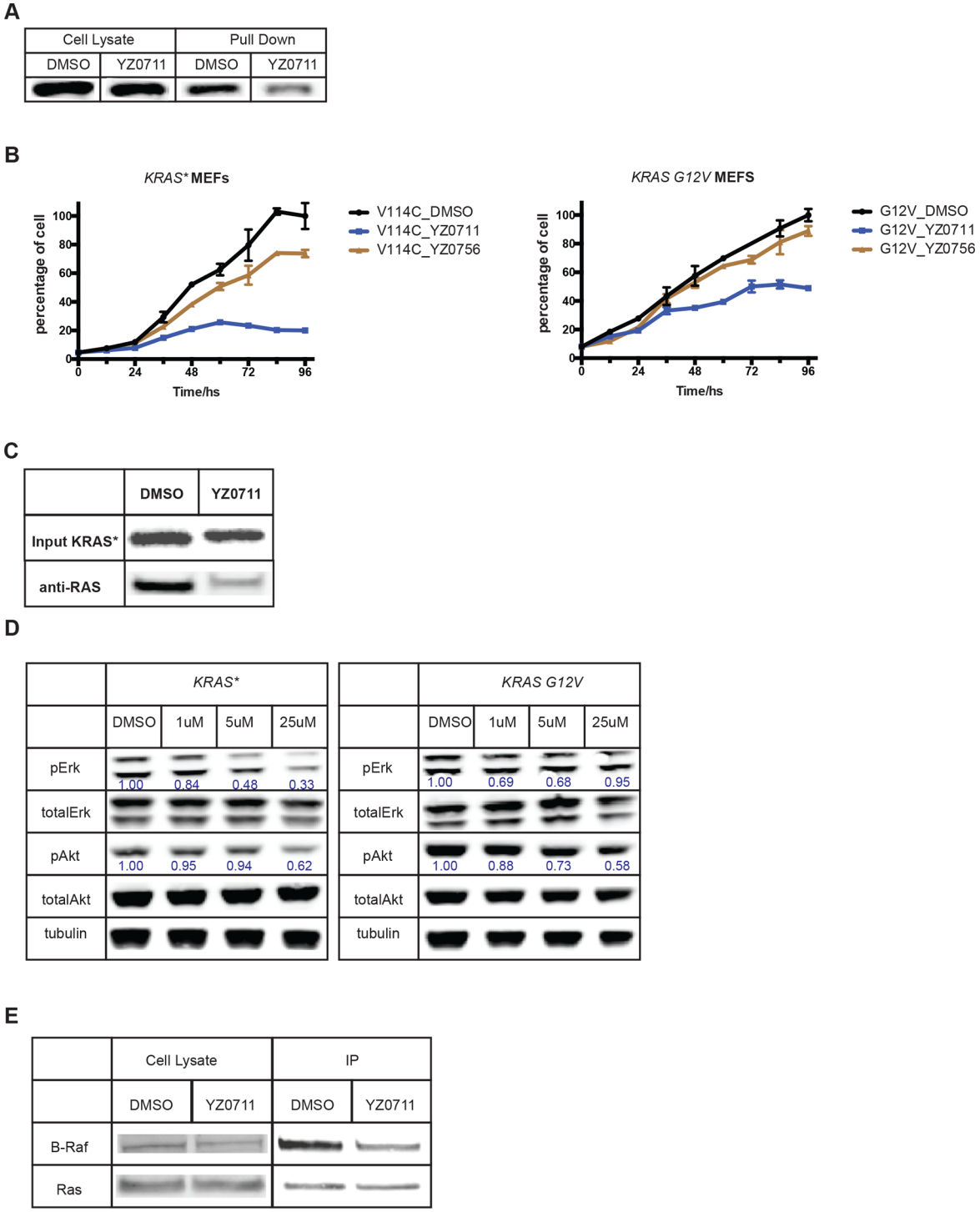

Figure 6. Compound YZ0711 activity in cells. (A) Desthiobiotin-GTP pull down. Treatment of *KRAS** MEFs with 100 μM YZ0711 for 6 h prior to probing with desthiobiotin-GTP decreases the amount of KRAS that can be pulled down with streptavidin compared to that in the control group. (B) Vi-cell assay. MEFs were treated with 25 μM YZ0711 or 25 μM YZ0756, and the cell density was measured every 12 h for 4 days. YZ0711 is more lethal to KRAS* MEFs than to KRAS G12V MEFs. (C) KRAS* was loaded with GTP first and then incubated with DMSO or compound YZ0711 for 15 min at room temperature, and the reaction was stopped by adding $MgCl_2$ (65 mM). Compound YZ0711 disrupted the binding of KRAS* to the RAF RBD. (D) MEFs were treated with DMSO and 1, 5, and 25 μM YZ0711 for 24 h. The pERK and pAKT levels were decreased in *KRAS** MEFs but not in *KRAS G12V* MEFs after the treatment with YZ0711. (E) Co-immunoprecipitation (IP) of B-RAF with RAS from the *KRAS** MEF cell line after treatment with compound YZ0711 (100 μM).

DOI: 10.1021/acs.biochem.7b01113
Biochemistry XXXX, XXX, XXX−XXX

whether the test compounds were able to penetrate cell membranes and covalently label KRAS*. Using LC−MS, we found that the level of accumulation of compound YZ0711 in *KRAS** MEFs was 1.4-fold compared to the compound concentration in the medium (Table S2). Desthiobiotin-GTP, which can covalently modify conserved lysine residues in the nucleotide-binding site, was used to pull down KRAS in cell lysates. *KRAS** MEFs treated with 50 μM YZ0711 have a decreased level of KRAS enrichment (Figure 6A), suggesting that YZ0711 is able to penetrate the cell membrane and target the GTP/GDP-binding site.

In a cell growth inhibition assay (Figure 6B and Figure S7), *KRAS** MEFs and $KRAS^{G12V}$ MEFs were treated with DMSO, 25 μM YZ0711, or 25 μM YZ0756 (a compound structurally similar to YZ0711) for 4 days and cell numbers were counted on a Vi-Cell XR Cell Viability Analyzer. Compound YZ0711 showed 80% inhibition of the *KRAS** MEF number and 50% inhibition of $KRAS^{G12V}$ MEFs, indicating that YZ0711 exhibits some off-target effect but is more selective for KRAS*. The cellular inhibition test using $BRAF^{V600E}$-*CAAX RASless* MEFs also indicated that compound YZ0711 selectively inhibits the growth of *KRAS** MEFs (Figure S7). Analogue YZ0756 exhibited 25% inhibition in *KRAS** MEFs and 15% inhibition in $KRAS^{G12V}$ MEFs, which is less potent than compound YZ0711.

Inhibition of the RAS Signaling Pathway. To test whether compound YZ0711 can disrupt KRAS*−effector binding, the RAF RBD protein, which can selectively pull down GTP-loaded KRAS*, was used. The GTP-loaded KRAS* protein was incubated with DMSO or YZ0711 (40 μM) for 15 min, the reaction stopped by the addition of $MgCl_2$ (65 mM), and then the mixture incubated with the RAF RBD protein. Minimal KRAS* was observed for YZ0711-bound KRAS* compared with GTP-loaded KRAS* (DMSO control group) (Figure 6C). To further investigate whether compound YZ0711 can inhibit the RAS/RAF/MEK/ERK and RAS/PI3K/AKT signaling pathways in cells, the phosphorylation levels of ERK and AKT were analyzed by a Western blot (Figure 6D). Treatment of *KRAS** MEFs with YZ0711 resulted in decreased pERK and pAKT levels. $KRAS^{G12V}$ MEFs were more resistant to this effect. Treatment of *KRAS** MEFs with YZ0711 also resulted in a decreased level of RAS-bound BRAF, suggesting YZ0711 can disrupt RAS signaling (Figure 6E).

DISCUSSION

Before embarking on a small-molecule drug discovery project directed against a specific target protein, it is critical to first validate the therapeutic effectiveness of the target in a specific disease, as well as the therapeutic index associated with target inhibition.[29] "Chemical" and "genetic" methods are two main approaches used in this target validation in which small molecules or genetic tools are used to modulate the target function.[30] Genetic methods including gene knockout and RNAi may have problems of generating null mutants for essential genes. Besides, in some cases there's a lack of alignment between RNAi and inhibitor studies, which mainly results from impairment of protein-protein interactions in RNAi study.[30] Small-molecule approaches can overcome the difficulties described above and provide additional information about druggability, toxicity, and the safety of inhibiting a target.

KRAS is an essential gene, and its gene product interacts with multiple upstream and downstream effectors. However, there is a lack of suitable chemical tools that can directly target KRAS. We developed a scalable system for testing the *in vitro* consequences of pharmacological inhibition of KRAS. An enlarged binding pocket was engineered into the GTP-binding site of KRAS through mutation of two conserved residues to alanine. The engineered KRAS is functionally distinguishable from $KRAS^{G12V}$ in the cell. We have designed and synthesized a small-molecule probe that covalently binds to an engineered KRAS mutant with high affinity and displaces GTP from the binding pocket. The probe allows selective binding to the engineered protein, but not the wild-type protein. The probe is also cell membrane-permeable and can selectively inhibit RAS signaling in cells. Covalent inhibitors are known to have off-target activity by forming a covalent bond with other proteins. We employed a chloroacetyl warhead, which has low intrinsic reactivity, to minimize this off-target effect.[24] The probe we designed is selective for the engineered KRAS but also has some extent of off-target effects in cells. The better selectivity and higher potency could be achieved by determining the co-crystal structure of the ligand−protein complex and further optimization of ligand structure and activity. The crystallization research is ongoing in our lab and will be reported in the future.

Small GTPases contribute to multiple cellular processes and different stages of cancer development and progression.[31−36] They have conserved GTP/GDP-binding pockets and share similar activation/deactivation mechanisms. Guanine nucleotide exchange factors (GEFs) catalyze the exchange of GDP with GTP, while GTPase-activating proteins (GAPs) accelerate the intrinsic GTPase activity of small GTPases. In the active state (GTP-bound state), small GTPases associate with a variety of effectors and promote downstream signaling. The system we designed here can be expanded for the design of allele selective small-molecule inhibitors of other proteins in the small GTPase family, thus providing tools for validating small GTPases. Considering the high affinity of small GTPases for GTP (nanomolar range) and the high concentration of GTP in cells (~0.5 mM),[22] a covalent inhibitor is generally necessary to compete with nucleotide binding. To achieve high selectivity and minimize the off-target effect, a targeted covalent inhibitor needs to be designed, which requires available protein crystal structures and structure−activity studies. In addition, choosing a protein that is easy to crystallize will be highly beneficial for the study.

ASSOCIATED CONTENT

Supporting Information

The Supporting Information is available free of charge on the ACS Publications website at DOI: 10.1021/acs.biochem.7b01113.

Five figures, three tables, LC−MS data, and methods (PDF)

AUTHOR INFORMATION

Corresponding Author

*Columbia University, Northwest Corner Building, 12th Floor, MC 4846, 550 W. 120th St., New York, NY 10027. E-mail: bstockwell@columbia.edu. Telephone: 212-854-2948. Fax: 212-854-2951.

ORCID

Brent R. Stockwell: 0000-0002-3532-3868

Funding

M.H.L. thanks for the fellowship from the Association pour la Recherche sur le Cancer (ARC) SAE20111204274 to M.-H.L. during her first year of postdoc training. This research was funded by National Institutes of Health Grants R21CA177591, R35CA209896, and P01CA087497 to B.R.S.

Notes

The authors declare no competing financial interest.

DOI: 10.1021/acs.biochem.7b01113
Biochemistry XXXX, XXX, XXX−XXX

REFERENCES

(1) Cromm, P. M., Spiegel, J., Grossmann, T. N., and Waldmann, H. (2015) Direct Modulation of Small GTPase Activity and Function. *Angew. Chem., Int. Ed. 54*, 13516.

(2) Cox, A. D., Fesik, S. W., Kimmelman, A. C., Luo, J., and Der, C. J. (2014) Drugging the undruggable RAS: Mission Possible? *Nat. Rev. Drug Discovery 13* (11), 828−51.

(3) Welsch, M. E., Kaplan, A., Chambers, J. M., Stokes, M. E., Bos, P. H., Zask, A., Zhang, Y., Sanchez-Martin, M., Badgley, M. A., Huang, C. S., Tran, T. H., Akkiraju, H., Brown, L. M., Nandakumar, R., Cremers, S., Yang, W. S., Tong, L., Olive, K. P., Ferrando, A., and Stockwell, B. R. (2017) Multivalent Small-Molecule Pan-RAS Inhibitors. *Cell 168* (5), 878−889.

(4) Ostrem, J. M., Peters, U., Sos, M. L., Wells, J. A., and Shokat, K. M. (2013) K-Ras(G12C) inhibitors allosterically control GTP affinity and effector interactions. *Nature 503* (7477), 548−51.

(5) Lim, S. M., Westover, K. D., Ficarro, S. B., Harrison, R. A., Choi, H. G., Pacold, M. E., Carrasco, M., Hunter, J., Kim, N. D., Xie, T., Sim, T., Janne, P. A., Meyerson, M., Marto, J. A., Engen, J. R., and Gray, N. S. (2014) Therapeutic targeting of oncogenic K-Ras by a covalent catalytic site inhibitor. *Angew. Chem., Int. Ed. 53* (1), 199−204.

(6) Bishop, A., Buzko, O., Heyeck-Dumas, S., Jung, I., Kraybill, B., Liu, Y., Shah, K., Ulrich, S., Witucki, L., Yang, F., Zhang, C., and Shokat, K. M. (2000) Unnatural ligands for engineered proteins: new tools for chemical genetics. *Annu. Rev. Biophys. Biomol. Struct. 29*, 577−606.

(7) Alaimo, P. J., Shogren-Knaak, M. A., and Shokat, K. M. (2002) Chemical Genetic Analysis of Protein Kinase Cascades. *Sci. World J. 2*, 108−110.

(8) Specht, K. M., and Shokat, K. M. (2002) The emerging power of chemical genetics. *Curr. Opin. Cell Biol. 14* (2), 155−9.

(9) Denzel, A., Hare, K. J., Zhang, C., Shokat, K., Jenkinson, E. J., Anderson, G., and Hayday, A. (2003) Cutting edge: a chemical genetic system for the analysis of kinases regulating T cell development. *J. Immunol. 171* (2), 519−23.

(10) Bishop, A. C., Zhang, X. Y., and Lone, A. M. (2007) Generation of inhibitor-sensitive protein tyrosine phosphatases via active-site mutations. *Methods 42* (3), 278−88.

(11) Coward, P., Wada, H. G., Falk, M. S., Chan, S. D., Meng, F., Akil, H., and Conklin, B. R. (1998) Controlling signaling with a specifically designed Gi-coupled receptor. *Proc. Natl. Acad. Sci. U. S. A. 95* (1), 352−7.

(12) Peet, D. J., Doyle, D. F., Corey, D. R., and Mangelsdorf, D. J. (1998) Engineering novel specificities for ligand-activated transcription in the nuclear hormone receptor RXR. *Chem. Biol. 5* (1), 13−21.

(13) Liberles, S. D., Diver, S. T., Austin, D. J., and Schreiber, S. L. (1997) Inducible gene expression and protein translocation using nontoxic ligands identified by a mammalian three-hybrid screen. *Proc. Natl. Acad. Sci. U. S. A. 94* (15), 7825−30.

(14) Clemons, P. A., Gladstone, B. G., Seth, A., Chao, E. D., Foley, M. A., and Schreiber, S. L. (2002) Synthesis of calcineurin-resistant derivatives of FK506 and selection of compensatory receptors. *Chem. Biol. 9* (1), 49−61.

(15) Belshaw, P. J., Schoepfer, J. G., Liu, K. Q., Morrison, K. L., and Schreiber, S. L. (1995) Rational Design of Orthogonal Receptor-Ligand Combinations. *Angew. Chem., Int. Ed. Engl. 34* (19), 2129−2132.

(16) Vincent, F., Cook, S. P., Johnson, E. O., Emmert, D., and Shah, K. (2007) Engineering unnatural nucleotide specificity to probe G protein signaling. *Chem. Biol. 14* (9), 1007−18.

(17) Fletcher, T. M., Cathers, B. E., Ravikumar, K. S., Mamiya, B. M., and Kerwin, S. M. (2001) Inhibition of human telomerase by 7-deaza-2'-deoxyguanosine nucleoside triphosphate analogs: potent inhibition by 6-thio-7-deaza-2'-deoxyguanosine 5'-triphosphate. *Bioorg. Chem. 29* (1), 36−55.

(18) Cool, R. H., Schmidt, G., Lenzen, C. U., Prinz, H., Vogt, D., and Wittinghofer, A. (1999) The Ras mutant D119N is both dominant negative and activated. *Mol. Cell. Biol. 19* (9), 6297−305.

(19) Walter, M., Clark, S. G., and Levinson, A. D. (1986) The oncogenic activation of human p21ras by a novel mechanism. *Science 233* (4764), 649−52.

(20) Wennerberg, K., Rossman, K. L., and Der, C. J. (2005) The Ras superfamily at a glance. *J. Cell Sci. 118* (5), 843−846.

(21) Hunter, J. C., Manandhar, A., Carrasco, M. A., Gurbani, D., Gondi, S., and Westover, K. D. (2015) Biochemical and Structural Analysis of Common Cancer-Associated KRAS Mutations. *Mol. Cancer Res. 13* (9), 1325−35.

(22) Ostrem, J. M., and Shokat, K. M. (2016) Direct small-molecule inhibitors of KRAS: from structural insights to mechanism-based design. *Nat. Rev. Drug Discovery 15* (11), 771−785.

(23) Drosten, M., Dhawahir, A., Sum, E. Y., Urosevic, J., Lechuga, C. G., Esteban, L. M., Castellano, E., Guerra, C., Santos, E., and Barbacid, M. (2010) Genetic analysis of Ras signalling pathways in cell proliferation, migration and survival. *EMBO J. 29* (6), 1091−104.

(24) Singh, J., Petter, R. C., Baillie, T. A., and Whitty, A. (2011) The resurgence of covalent drugs. *Nat. Rev. Drug Discovery 10* (4), 307−17.

(25) Zhu, K., Borrelli, K. W., Greenwood, J. R., Day, T., Abel, R., Farid, R. S., and Harder, E. (2014) Docking covalent inhibitors: a parameter free approach to pose prediction and scoring. *J. Chem. Inf. Model. 54* (7), 1932−40.

(26) Krishnamurty, R., Brock, A. M., and Maly, D. J. (2011) Protein kinase affinity reagents based on a 5-aminoindazole scaffold. *Bioorg. Med. Chem. Lett. 21* (1), 550−4.

(27) Abel, R., Young, T., Farid, R., Berne, B. J., and Friesner, R. A. (2008) Role of the active-site solvent in the thermodynamics of factor Xa ligand binding. *J. Am. Chem. Soc. 130* (9), 2817−31.

(28) Young, T., Abel, R., Kim, B., Berne, B. J., and Friesner, R. A. (2007) Motifs for molecular recognition exploiting hydrophobic enclosure in protein-ligand binding. *Proc. Natl. Acad. Sci. U. S. A. 104* (3), 808−13.

(29) Carney, S. (2012) Target validation. *Drug Discovery Today 17*, S1−S2.

(30) Weiss, W. A., Taylor, S. S., and Shokat, K. M. (2007) Recognizing and exploiting differences between RNAi and small-molecule inhibitors. *Nat. Chem. Biol. 3* (12), 739−744.

(31) Nishikimi, A., Uruno, T., Duan, X., Cao, Q., Okamura, Y., Saitoh, T., Saito, N., Sakaoka, S., Du, Y., Suenaga, A., Kukimoto-Niino, M., Miyano, K., Gotoh, K., Okabe, T., Sanematsu, F., Tanaka, Y., Sumimoto, H., Honma, T., Yokoyama, S., Nagano, T., Kohda, D., Kanai, M., and Fukui, Y. (2012) Blockade of inflammatory responses by a small-molecule inhibitor of the Rac activator DOCK2. *Chem. Biol. 19* (4), 488−97.

(32) Montalvo-Ortiz, B. L., Castillo-Pichardo, L., Hernandez, E., Humphries-Bickley, T., De la Mota-Peynado, A., Cubano, L. A., Vlaar, C. P., and Dharmawardhane, S. (2012) Characterization of EHop-016, novel small molecule inhibitor of Rac GTPase. *J. Biol. Chem. 287* (16), 13228−38.

(33) Shang, X., Marchioni, F., Sipes, N., Evelyn, C. R., Jerabek-Willemsen, M., Duhr, S., Seibel, W., Wortman, M., and Zheng, Y. (2012) Rational Design of Small Molecule Inhibitors Targeting RhoA Subfamily Rho GTPases. *Chem. Biol. 19* (6), 699−710.

(34) Nassar, N., Cancelas, J., Zheng, J., Williams, D. A., and Zheng, Y. (2006) Structure-function based design of small molecule inhibitors targeting Rho family GTPases. *Curr. Top. Med. Chem. 6* (11), 1109−16.

(35) Vigil, D., Cherfils, J., Rossman, K. L., and Der, C. J. (2010) Ras superfamily GEFs and GAPs: validated and tractable targets for cancer therapy? *Nat. Rev. Cancer 10* (12), 842−57.

(36) Vega, F. M., and Ridley, A. J. (2008) Rho GTPases in cancer cell biology. *FEBS Lett. 582* (14), 2093−101.

DOI: 10.1021/acs.biochem.7b01113
Biochemistry XXXX, XXX, XXX−XXX